

AD-A170 135

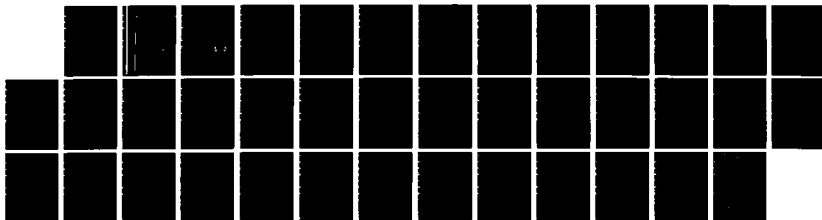
THE THREE DIMENSIONAL STRESS INTENSITY FACTOR DUE TO
THE MOTION OF A LOAD (U) BROWN UNIV PROVIDENCE RI DIV
OF ENGINEERING J RAMIREZ MAY 86 N00044-85-K-0597

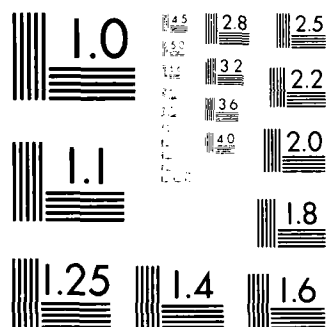
1/1

UNCLASSIFIED

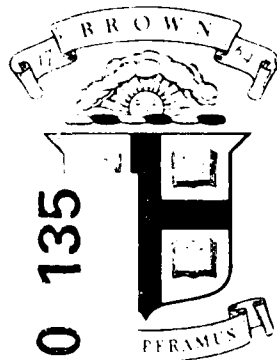
F/G 20/11

NL





MICROCOPY RESOLUTION TEST CHART
NATIONAL BUREAU OF STANDARDS-1963-A



AD-A170 135

mic file copy

Brown University

DIVISION OF ENGINEERING

PROVIDENCE, R.I. 02912

THE THREE DIMENSIONAL STRESS INTENSITY
FACTOR DUE TO THE MOTION OF A LOAD
ON THE FACES OF A CRACK

by

Jean-Claude Ramirez
Division of Engineering
Brown University
Providence, RI 02912 USA

DTIC
ELECTE
JUL 25 1986
S D

This document has been approved
for public release and sale; its
distribution is unlimited.

86 7 8 009

THE THREE DIMENSIONAL STRESS INTENSITY
FACTOR DUE TO THE MOTION OF A LOAD
ON THE FACES OF A CRACK

by

Jean-Claude Ramirez
Division of Engineering
Brown University
Providence, RI 02912 USA

DTIC
ELECTE
JUL 25 1986
S D

NATIONAL SCIENCE FOUNDATION
Grant MSM-85-13096

OFFICE OF NAVAL RESEARCH
Contract N00014-85-k-0597

May 1986

**THE THREE DIMENSIONAL STRESS INTENSITY FACTOR
DUE TO THE MOTION OF A LOAD
ON THE FACES OF A CRACK**

Jean-Claude Ramirez
Division of Engineering
Brown University
Providence, RI 02912 USA

ABSTRACT

The dynamic stress intensity factor history for a half plane crack in an otherwise unbounded elastic body, with the crack faces subjected to a traction distribution consisting of a pair of point loads that move in a direction perpendicular to the crack edge, is considered. The exact expression for the mode I stress intensity factor as a function of time for any point along the crack edge is obtained by extending a procedure recently introduced by Freund [1]. The method of solution is based on integral transforms methods and the theory of analytic functions of a complex variable. Some features of the solution are discussed and graphical results for various point load speeds are presented.



Accession For	
NTIS CRA&I	<input checked="checked" type="checkbox"/>
DTIC TAB	<input type="checkbox"/>
Unannounced	<input type="checkbox"/>
Justification	
By	
Distribution/	
Availability Codes	
Dist	Avail and/or Special
A-1	

1. INTRODUCTION

A general procedure has been introduced by Freund [1] for determining the stress intensity factor histories for a class of three dimensional elastodynamic crack problems. As an illustration of the procedure, Freund studied a half plane crack in an otherwise unbounded elastic solid, with the crack faces subjected to a pair of line loads that are suddenly applied along a line perpendicular to the crack front. Because the approach is novel, its range of applicability has not yet been established. Here, the extension of the procedure to situations with moving loads on the crack faces is considered. This distribution consists of a pair of point loads that suddenly begins to act at the edge of the crack, and moves at a constant velocity along the crack faces in a direction perpendicular to the crack edge. The corresponding two dimensional problem was studied by Ang [2]. A three dimensional problem that is related to the one in this paper is that of a point load traveling on the surface of an elastic half space. This problem was analyzed by Gakenheimer and Miklowitz [3], who considered all point load speeds, i.e. subsonic, transonic and supersonic. For the purposes of this paper, attention is restricted to subsonic point load speeds, that is, the speed is less than the characteristic Rayleigh wave speed of the material. The analysis for higher speeds offers no added mathematical difficulty.

In section 2, the general formulation of the boundary value problem is presented for the three dimensional crack face tractions resulting in mode

I deformation. Section 3 describes the general approach to solving the problem by means of transform methods. In section 4, the formal solution to the particular traction distribution is obtained by means of the Wiener-Hopf decomposition method. In section 5 the dynamic stress intensity factor history is extracted by making use of the asymptotic properties of transforms, the Cagniard-deHoop method, and the convolution theorem for transforms. A discussion of the results is given in section 6.

2. GENERAL FORMULATION

In vector notation the Navier equation governing the displacement vector \mathbf{u} for an isotropic elastic solid is written as

$$\ddot{\mathbf{u}} = c_l^2 \nabla(\nabla \cdot \mathbf{u}) - c_s^2 \nabla \times (\nabla \times \mathbf{u}) \quad (2.1)$$

where c_l and c_s are the dilational and shear wave speeds, respectively. In terms of the Lamé constants λ and μ and the mass density ρ , the wave speeds are given by

$$c_l^2 = (\lambda + 2\mu)/\rho, \quad c_s^2 = \mu/\rho. \quad (2.2)$$

It is also useful to introduce the dilatational and shear slownesses a and b , where $a = 1/c_l$ and $b = 1/c_s$. Furthermore, the Rayleigh wave speed of the elastic material is denoted by c_r and its corresponding slowness by r .

A standard approach when solving (2.1) is to introduce the displacement potentials ϕ and ψ through the Helmholtz decomposition of the displacement vector, i.e.

$$\mathbf{u} = \nabla\phi + \nabla \times \psi, \quad \nabla \cdot \psi = 0. \quad (2.3)$$

The scalar potential ϕ is called the dilatational potential and the vector

potential Ψ is the shear potential. The divergence free requirement on the shear potential is necessary in order to make the decomposition unique. The advantage of this decomposition is that the potentials ϕ and Ψ satisfy the uncoupled wave equations

$$\ddot{\phi} = c_l^2 \nabla^2 \phi, \quad \ddot{\Psi} = c_s^2 \nabla^2 \Psi. \quad (2.4)$$

The linear differential equations (2.4) have the added advantage of lending themselves to standard integral transform methods. The two potentials are coupled through the boundary conditions that characterize the problem to be described.

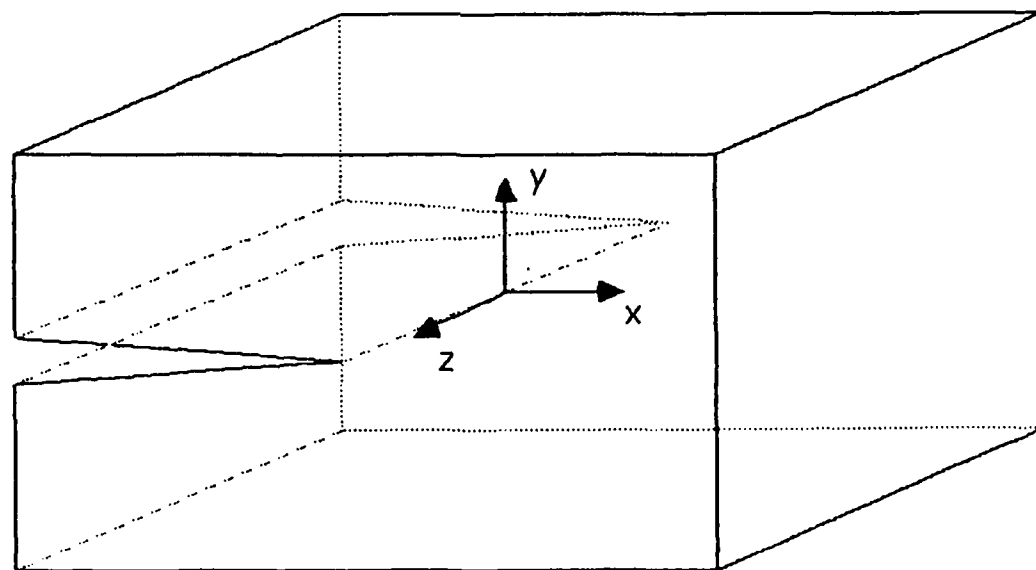


Figure 1. Geometrical configuration of the elastic solid.

Consider the elastic body containing a half plane crack depicted in Figure 1. A right handed rectangular coordinate system is introduced such that the z axis coincides with the crack front, and the half plane crack occupies the region $y=0, x<0$. Attention is restricted to applied tractions of the form $T_y = \mp \sigma_{\pm}(x,z,t)$ on $y = \pm 0$ where $\sigma_{\pm} > 0$ corresponds to a tensile traction. All other components of the imposed traction are zero. The function σ_{\pm} is prescribed for $x < 0$ and is extended so that $\sigma_{\pm} \equiv 0$ in the half range $x > 0$. The minus subscript is used to denote a function that is nonvanishing in the range $x < 0$. Likewise, the plus subscript will be used to label functions that are nonzero in the half range $x > 0$, but are identically zero for $x < 0$. This notation is useful in problems like this one, where the transforms of these "half functions" turn out to be analytic functions of the transform parameter in lower (minus) and upper (plus) half planes.

Due to the symmetry of the geometry and the applied traction, the displacement fields satisfy the following conditions:

$$\begin{aligned} u_x(x, -y, z, t) &= u_x(x, y, z, t) \\ u_y(x, -y, z, t) &= -u_y(x, y, z, t) \\ u_z(x, -y, z, t) &= u_z(x, y, z, t). \end{aligned} \tag{2.5}$$

Thus attention can be restricted to the upper half space $y \geq 0$.

Furthermore, properties (2.5) imply that $\sigma_{xy}(x,0,z,t)$ and $\sigma_{yz}(x,0,z,t)$ vanish for all z and t , and that $u_y(x,0,z,t) = u_-(x,z,t)$ where u_- represents the unknown y component of the displacement on the crack faces for $x < 0$ and $u_- \equiv 0$ in the half range $x > 0$. Hence, the complete set of boundary conditions to be satisfied by the stress field is

$$\begin{aligned}\sigma_{yy}(x,0,z,t) &= \sigma_-(x,z,t) + \sigma_+(x,z,t) \\ \sigma_{xy}(x,0,z,t) &= 0 \\ \sigma_{yz}(x,0,z,t) &= 0 \\ u_y(x,0,z,t) &= u_-(x,z,t)\end{aligned}\tag{2.6}$$

for $-\infty < x, z < \infty$ and $0 \leq t$. The function σ_+ represents the unknown normal component of stress σ_{yy} on $x > 0$, and $\sigma_+ \equiv 0$ for $x < 0$.

The initial conditions are that the material is stress free and at rest for $t \leq 0$. These are expressed in terms of the displacement potentials by

$$\varphi(x,y,z,0) = \partial_t \varphi(x,y,z,0) = \psi(x,y,z,0) = \partial_t \psi(x,y,z,0) = 0 \tag{2.7}$$

for $y > 0$. Likewise, the boundary conditions (2.6) can be replaced by their corresponding representations in terms of φ and ψ , which are

$$\begin{aligned}
& \lambda \nabla^2 \phi + 2\mu \{ \partial_{yy} \phi + \partial_y [\partial_z \psi_x - \partial_x \psi_z] \} = \sigma_- + \sigma_+ \\
& 2\partial_{xy} \phi + \partial_y [\partial_y \psi_z - \partial_z \psi_y] + \partial_x [\partial_z \psi_x - \partial_x \psi_z] = 0 \\
& 2\partial_{yz} \phi + \partial_z [\partial_z \psi_x - \partial_x \psi_z] + \partial_y [\partial_x \psi_y - \partial_y \psi_x] = 0 \\
& \partial_y \phi + \partial_z \psi_x - \partial_x \psi_z = u_-
\end{aligned} \tag{2.8}$$

for $-\infty < x, z < \infty$ and $0 \leq t$. ψ_x , ψ_y and ψ_z are the rectangular cartesian components of ψ .

3. TRANSFORMS

In order to solve the problem described by the partial differential equations (2.4), the initial conditions (2.7), and the boundary conditions (2.8), use is made of Laplace and Fourier transforms. First, the one-sided Laplace transform is applied to the differential equations and the boundary conditions, and the initial conditions are imposed. This Laplace transform in time has the transform parameter s , and is denoted by a superposed hat. For a function $\varphi(x,y,z,t)$ this transform is given by

$$\hat{\varphi}(x,y,z,s) = \int_0^{\infty} \varphi(x,y,z,t) e^{-st} dt. \quad (3.1)$$

For the time being, s is taken to be real and large enough so as to be on the right of the abscissa of convergence of the integral. The dependence on z and x is then suppressed by applying a pair of two-sided Fourier transforms. These transforms have the transform parameters $i\zeta s$ and $i\xi s$, respectively. They are denoted, respectively, by the upper case symbol for the function with a superposed hat, and the upper case symbol itself, to wit,

$$\begin{aligned} \hat{\Phi}(x,y,\zeta,s) &= \frac{1}{\sqrt{2\pi}} \int_{-\infty}^{\infty} \hat{\varphi}(x,y,z,s) e^{is\zeta z} dz \\ \Phi(\xi,y,\zeta,s) &= \frac{1}{\sqrt{2\pi}} \int_{-\infty}^{\infty} \hat{\Phi}(x,y,\zeta,s) e^{is\xi x} dx. \end{aligned} \quad (3.2)$$

The introduction of the s parameter into the kernel of the transforms (3.2)

is for algebraic convenience; it takes care of a change of variables that would otherwise be needed at a later point in the analysis.

Due to the wave propagation character of the solution, the strip of analyticity of the Fourier transforms can be anticipated. Suppose that the applied tractions are such that σ_- vanishes for $|z| > z_0$. Then, at any given time t , the region of causality is confined to $|z| < z_0 + tc_1$. Thus by considering the elementary wave field $\phi = H[t + (z + z_0)a] + H[t - (z - z_0)a]$, where $H(\cdot)$ is Heaviside's unit function, and applying to it the Laplace transform, one obtains

$$\hat{\phi} = O(e^{-s(|z| - z_0)a}) \text{ as } |z| \uparrow \infty. \quad (3.3)$$

This, in turn, implies that the Fourier transform $\hat{\phi}$ converges for the strip $|\text{Im}(\zeta)| < a$. Thus $\hat{\phi}$ defines an *analytic* function of ζ in the strip of convergence. Consequently, one can analytically continue $\hat{\phi}$ to values of ζ that are not contained in the strip of convergence. At this point in the analysis it is convenient to restrict ζ to this strip. The identity property of analytic functions [4], allows one to restrict ζ to the portion of the imaginary axis in the interval $-a < \text{Im}(\zeta) < a$, $\text{Re}(\zeta) = 0$. The idea is to perform the Wiener-Hopf factorization in the ζ plane only, keeping ζ confined to the strip of analyticity of $\hat{\phi}$. At a later point in the analysis it will be essential to analytically extend functions of ζ away from the interval on the imaginary axis and outside the strip.

The domain of convergence of the Fourier transform in x can also be anticipated. Suppose that the applied tractions are such that along the crack faces σ_- is nonzero for indefinitely large values of x in the negative direction. Then, in this region the integral Φ will converge provided that $\text{Im}(\xi) < 0$. On the other hand, by definition the applied tractions do not extend along the positive x direction and thus, the region of causality does not extend beyond a certain cylindrical wavefront ahead of the crack front. To be precise, for $x > 0$, the front is centered at the y axis and at any given time t , has a radius $z_0 + (x^2 + z^2)^{1/2}$. Thus, by considering the elementary wave field $\psi = H(t - (z_0 + \sqrt{x^2 + z^2})/a)$ and applying to it the transforms (3.1) and (3.2) it is found that the final integral converges if $\{\text{Im}(\xi)\}^2 - \zeta^2 < a^2$. Therefore the Fourier integral Φ defines an analytic function in the strip $-\sqrt{\zeta^2 + a^2} < \text{Im}(\xi) < 0$ in the ξ plane, with ζ restricted to $-a < \text{Im}(\zeta) < a$, $\text{Re}(\zeta) = 0$.

The class of problems which is accessible by the solution procedure outlined in the Introduction, is one in which $\sigma_-(x, z, t)$ is restricted to having a triple transform which has the separable form,

$$\frac{1}{2\pi} \int_{-\infty}^{\infty} \int_{-\infty}^{\infty} \hat{\sigma}_-(x, z, s) e^{is(\xi x + \zeta z)} dz dx = \frac{1}{s^m} \Sigma_-(\xi, \zeta) \quad (3.4)$$

where m is a real number and $\Sigma_-(\xi, \zeta)$ does not depend on s . The reason for this will be more apparent in section 5. The requirement (3.4) makes it

possible to perform the final inversion of the dynamic stress intensity factor by means of the convolution formula for Laplace transforms.

The application of the transforms (3.1) and (3.2) to the partial differential equations (2.4) reduces them to ordinary differential equations,

$$\frac{\partial^2 \Phi}{\partial y^2} - s^2 \alpha^2 \Phi = 0 \quad \text{and} \quad \frac{\partial^2 \Psi}{\partial y^2} - s^2 \beta^2 \Psi = 0 \quad (3.5)$$

where

$$\alpha = \alpha(\zeta, \xi) = \sqrt{\zeta^2 + \xi^2 + a^2} \quad , \quad \beta = \beta(\zeta, \xi) = \sqrt{\zeta^2 + \xi^2 + b^2} \quad (3.6)$$

and $a=1/c_l$, $b=1/c_s$ are the dilatational and shear slowneses introduced after (2.2). The complex ξ plane is cut along $\sqrt{a^2 + \zeta^2} < |\text{Im}(\xi)| < \infty$, $\text{Re}(\xi) = 0$ and $\sqrt{b^2 + \zeta^2} < |\text{Im}(\xi)| < \infty$, $\text{Re}(\xi) = 0$ so that $\text{Re}(\alpha) \geq 0$ and $\text{Re}(\beta) \geq 0$ in the cut plane for each admissible value of ζ . With the ξ plane cut in this fashion, equations of the type (3.5) have the solutions, bounded as $y \rightarrow \infty$ to preclude waves coming in from remote regions,

$$\Phi = \frac{A(\xi, \zeta)}{s^{m+2}} e^{-s\alpha y} \quad , \quad \Psi = \frac{\Theta(\xi, \zeta)}{s^{m+2}} e^{-s\beta y} \quad (3.7)$$

where $\Theta = \{B(\xi, \zeta), C(\xi, \zeta), D(\xi, \zeta)\}$.

Transforming the condition $\nabla \cdot \Psi = 0$ yields

$$\xi B - i\beta C + \zeta D = 0. \quad (3.8)$$

It is also necessary to transform the boundary conditions (2.8), which will yield four more equations. They are

$$\begin{aligned} (b^2 + 2\xi^2 + 2\zeta^2)A + 2i\zeta\beta B - 2i\xi\beta D &= \mu^{-1}(\Sigma_- + \Sigma_+) \\ 2i\xi\alpha A - \xi\zeta B - i\zeta\beta C + (\beta^2 + \xi^2)D &= 0 \\ 2i\zeta\alpha A - (\beta^2 + \zeta^2)B + i\xi\beta C + \xi\zeta D &= 0 \\ -\alpha A - i\zeta B + i\xi D &= U_- . \end{aligned} \quad (3.9)$$

In reducing the equations to this form use is made of the fact that $\lambda c_d^{-2} = \mu(b^2 - 2a^2)$. Furthermore we have defined U_- and Σ_+ as

$$\begin{aligned} U_-(\xi, \zeta) &= \frac{s^{m+1}}{2\pi} \int_{-\infty}^{\infty} \int_{-\infty}^{\infty} \hat{U}_-(x, z, s) e^{is(\xi x + \zeta z)} dz dx \\ \Sigma_+(\xi, \zeta) &= \frac{s^m}{2\pi} \int_{-\infty}^{\infty} \int_{-\infty}^{\infty} \hat{\sigma}_-(x, z, s) e^{is(\xi x + \zeta z)} dz dx . \end{aligned} \quad (3.10)$$

The parameter s is absent, by construction, from the five equations (3.8) and (3.9). There are six unknown parameters, four constants of integration A, B, C, D and two sectionally analytic functions U_- and Σ_+ , but only five equations to relate them. One can solve for the four constants of integration in terms of the two unknown sectionally analytic functions.

The result is

$$\begin{aligned}
 A(\xi, \zeta) &= \alpha^{-1}(1 - 2\beta^2 b^{-2})U_-(\xi, \zeta) \\
 B(\xi, \zeta) &= -2i\zeta b^{-2}U_-(\xi, \zeta) \\
 C(\xi, \zeta) &= 0 \\
 D(\xi, \zeta) &= 2i\xi b^{-2}U_-(\xi, \zeta).
 \end{aligned} \tag{3.11}$$

Substituting for these functions into the first equation of (3.9) we obtain one equation relating the two unknown functions,

$$-\frac{\mu}{b^2 \alpha} R(\xi, \zeta) U_-(\xi, \zeta) = \Sigma_-(\xi, \zeta) + \Sigma_+(\xi, \zeta) \tag{3.12}$$

where

$$R(\xi, \zeta) = [b^2 + 2(\xi^2 + \zeta^2)]^2 - 4(\xi^2 + \zeta^2)\alpha(\xi, \zeta)\beta(\xi, \zeta). \tag{3.13}$$

This is the modified Rayleigh wave function, that is, it corresponds to the standard Rayleigh wave function, $R(z)$, when $\zeta=0$. It is a well established fact [5] that the standard Rayleigh wave function, in a properly cut z plane, has only two zeros, $R(\pm ir)=0$ where $r=1/c_r$. Thus, the modified Rayleigh wave function in the properly cut complex ξ plane only has the two zeros $\xi = \pm i\bar{r}$, where $\bar{r} = \sqrt{\zeta^2 + r^2}$.

Equation (3.12) is a standard Wiener-Hopf equation, and the essence of

the Wiener-Hopf method is to solve for the two unknown sectionally analytic functions U_- and Σ_+ from a single equation (3.12). The approach to be followed in section 4 is actually due to Jones [6]. Since Σ_+ is analytic in the half plane $\text{Im}(\xi) > -\sqrt{\xi^2 + a^2}$, and U_- is analytic in the half plane $\text{Im}(\xi) < 0$, (3.12) holds in the strip $-i\sqrt{\xi^2 + a^2} < \xi < 0$. Furthermore, ζ is restricted to the interval $-a < \text{Im}(\zeta) < a$, $\text{Re}(\zeta) = 0$, so for a fixed value of ζ (3.12) can be solved by factorization in the ξ plane alone.

4. FORMAL SOLUTION

At this point it is necessary to introduce the particular applied traction distribution. The present work is concerned with a pair of point loads that suddenly begins to act at the edge of the crack $x=y=z=0$ and moves in the negative x direction, i.e. perpendicular to the crack edge, at a constant velocity v . Thus, we assume that

$$\sigma_-(x,z,t) = -P\delta(z)\delta(x+vt) \quad 0 < v < c_r \quad (4.1)$$

where $\delta(\cdot)$ is Dirac's delta function. The amplitude P has physical dimensions of force and $P > 0$ corresponds to a traction that tends to separate the crack faces.

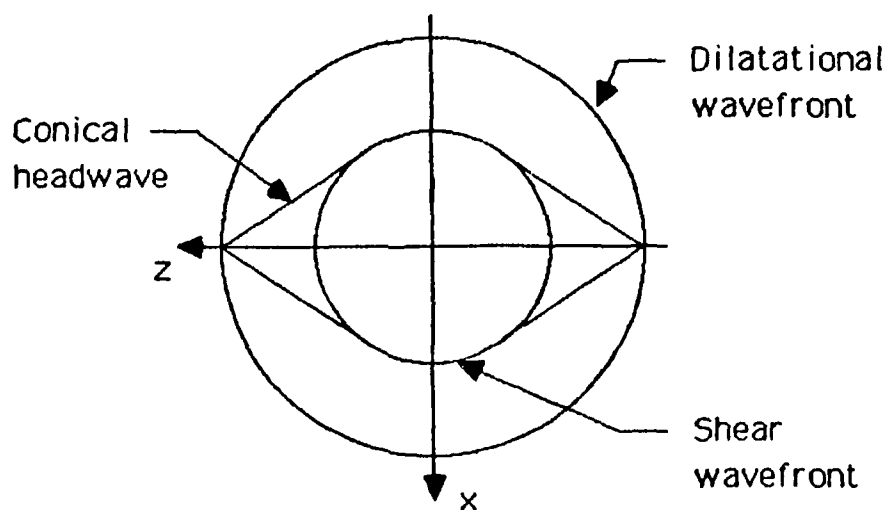


Figure 2. Traces in the x - z plane of the wavefronts resulting from the application of the tractions (4.1).

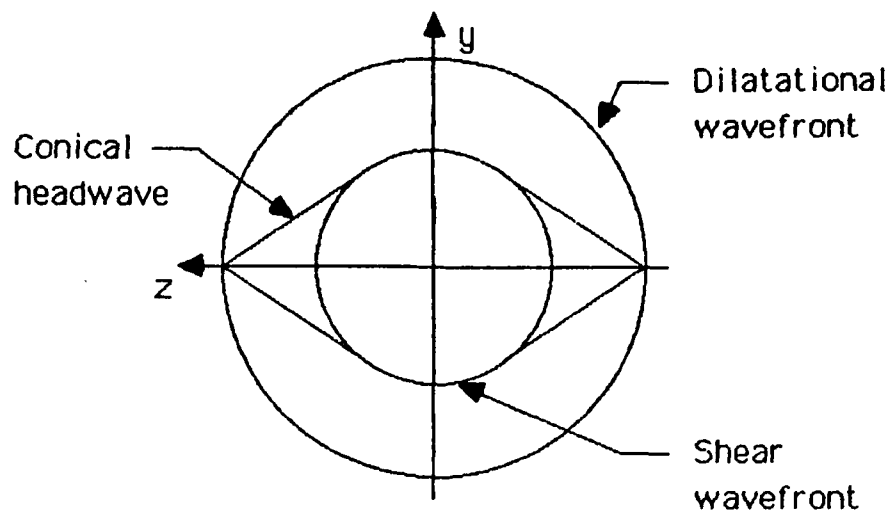


Figure 3. Traces in the y - z plane of the wavefronts resulting from the application of the tractions (4.1).

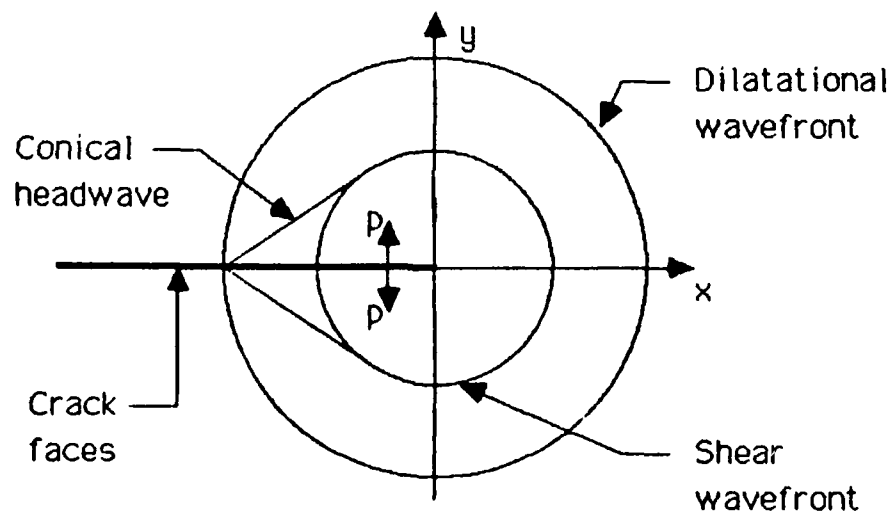


Figure 4. Traces in the x - y plane of the wavefronts resulting from the application of the tractions (4.1).

Figures 2, 3 and 4 indicate the leading wavefronts that result from the application of the tractions (4.1). These wavefronts have been obtained by extrapolation from experience with two dimensional problems in hyperbolic partial differential equations rather than by solving for the displacement

potentials. The wavefronts include spherical dilatational and shear wavefronts centered at the origin of coordinates (Fig. 2). There are also two sets of headwaves that form cones with vertices where the spherical dilatational front meets the z axis, and extend to circles of tangency with the spherical shear wavefront. The traces of these cones which extend to the crack faces, as well as ahead of the crack edge, are shown in Figure 2. Furthermore, there are conical headwaves that intersect the dilatational wavefronts on the surfaces $y = \pm 0$ for $x < 0$, and extend to circles of tangency with the spherical shear wavefronts (Figs. 3 and 4). The headwaves arise since the dilatational waves alone cannot satisfy the traction free boundary conditions that exist at the crack faces.

Transforming (4.1) with (3.1) and (3.2), it is found that $m=1$ and that

$$\Sigma_-(\xi, \zeta) = \frac{iP}{2\pi v} \frac{1}{(\zeta - ic)} \quad (4.2)$$

where $c = 1/v$ is the point load slowness. Substituting for $\Sigma_-(\xi, \zeta)$ in (3.12) one obtains the Wiener-Hopf equation that corresponds to the problem with traction loading (4.1),

$$-\frac{\mu}{b^2 \alpha} R(\xi, \zeta) U_-(\xi, \zeta) = \frac{iP}{2\pi v} \frac{1}{(\zeta - ic)} + \Sigma_+(\xi, \zeta). \quad (4.3)$$

Only some of the steps involved in the factorization of (4.3) in the ξ plane will be shown below. To begin, let $\bar{a}^2 = \zeta^2 + a^2$ and note \bar{a} is some

constant in the interval $(0, a)$ since ζ is being held fixed in the interval $(-ia, ia)$. The function α can be factorized as,

$$\alpha(\xi; \zeta) = (\xi^2 + \bar{a}^2)^{1/2} = [(\xi + i\bar{a})^{1/2}]_+ [(\xi - i\bar{a})^{1/2}]_- . \quad (4.4)$$

The semicolon is used to emphasize the fact that ζ is being held fixed and its influence in the factorization procedure is only parametric in nature. The plus (minus) subscript is used to denote functions that are analytic in the upper (lower) half plane $\text{Im}(\xi) > -\bar{a} (< 0)$. The fact that the two planes overlap is no coincidence. Indeed, for (3.12) or (4.3) to have useful consequences there must be a common strip in which Σ_+ and U_- exist. In problems of this sort, one *hopes* that σ_+ and u_- are such that the inversion paths of their Fourier transforms satisfy the above requirement, and proceeds, verifying the initial assumption *a posteriori*.

In order to make further progress one must factorize the Rayleigh wave function $R(\xi; \zeta)$. For this purpose it is most convenient to express $R(\xi; \zeta)$ in terms of a function with neither zeroes nor poles and whose limiting value as $|\xi| \uparrow \infty$ is unity ([6], pp. 13-15). Such a function is easily constructed from the asymptotic properties of the Rayleigh wave function and knowledge of its roots. Specifically, one must make use of the results that

$$R(\xi; \zeta) = 2\xi^2(b^2 - a^2) + O(1) \text{ as } |\xi| \uparrow \infty \quad (4.5)$$

and $R(\xi; \zeta)$ has two symmetric roots $\xi = \pm i\bar{r}$, where $\bar{r} = \sqrt{\zeta^2 + r^2}$, as discussed at the end of section 3. The function needed is easily seen to be

$$S(\xi; \zeta) = \frac{R(\xi; \zeta)}{\kappa(\bar{r}^2 + \xi^2)} \quad (4.6)$$

where $\kappa = 2(b^2 - a^2)$. The function S has the required properties of being nonvanishing in the finite ξ plane and being asymptotic to unity for large values of ξ . In the Appendix it is shown that $S(\xi; \zeta)$ can be factorized as $S_+(\xi; \zeta)S_-(\xi; \zeta)$ where

$$S_{\pm}(\xi, \zeta) = \exp \left\{ \frac{1}{\pi} \int_a^b \tan^{-1} \left[\frac{4\eta^2 \sqrt{(b^2 - \eta^2)(\eta^2 - a^2)}}{(b^2 - 2\eta^2)^2} \right] \frac{\eta d\eta}{\sqrt{\zeta^2 + \eta^2} (\sqrt{\zeta^2 + \eta^2} \pm \xi)} \right\}. \quad (4.7)$$

The functions $S_+(\zeta, \zeta)$ and $S_-(\xi; \zeta)$ are analytic and nonzero in the half planes $\text{Im}(\xi) > -\bar{a}$ and $\text{Im}(\xi) < \bar{a}$.

After some straight-forward manipulations, (4.3) can be rewritten as

$$-\frac{\mu \kappa U_-(\xi; \zeta)}{b^2 G_-(\xi; \zeta)} = \left[\frac{iP}{2\pi v(\xi - ic)} + \Sigma_+(\xi; \zeta) \right] G_+(\xi; \zeta) \quad (4.8)$$

where

$$G_{\pm}(\xi; \zeta) = \frac{(\xi \pm i\bar{a})^{1/2}}{(\xi \pm i\bar{r})S_{\pm}(\xi; \zeta)} \quad (4.9)$$

At this point the factorization is almost complete. It remains to remove the pole in $G_{+}(\xi; \zeta)$ at $\xi = ic$. This is accomplished by observing that

$$\frac{G_{+}(\xi; \zeta)}{\xi - ic} = \left[\frac{G_{+}(\xi; \zeta) - G_{+}(ic; \zeta)}{\xi - ic} \right]_{+} + \left[\frac{G_{+}(ic; \zeta)}{\xi - ic} \right]_{-} \quad (4.10)$$

Now the factorization is complete and relationship (4.8) may be rewritten as

$$-\frac{\mu\kappa}{b^2} \frac{U_{-}(\xi; \zeta)}{G_{-}(\xi; \zeta)} - \frac{iP}{2\pi\nu} \frac{G_{+}(ic; \zeta)}{(\xi - ic)} = \frac{iP}{2\pi\nu} \frac{[G_{+}(\xi; \zeta) - G_{+}(ic; \zeta)]}{(\xi - ic)} + G_{+}(\xi; \zeta)\Sigma_{+}(\xi; \zeta). \quad (4.11)$$

The function on the left hand side of (4.11) is analytic in the half plane $\text{Im}(\xi) < 0$. The function on the right hand side is analytic in the half plane $\text{Im}(\xi) > -i\sqrt{\zeta^2 + a^2}$. Since (4.11) holds in the strip where the domains of analyticity of the two functions overlap, the functions are each analytic continuations of the other. Together they define an entire function $E(\xi)$ ([6], p. 37). The function $E(\xi)$ is to be determined from the behaviour of the functions U_{-} , Σ_{+} and G_{\pm} as $|\xi| \uparrow \infty$.

For the class of fracture mechanics problems described in section 2, the normal stress σ_+ on the plane $y=0$ is expected to have the asymptotic behavior

$$\sigma_+(x,z,t) \sim k_I(t,z)/\sqrt{2\pi x} \quad \text{as } x \downarrow 0^+ \quad (4.12)$$

where $k_I(t,z)$ is the dynamic stress intensity factor history at any point along the crack front. This history will be determined explicitly in the next section. In light of (4.12), $\hat{\sigma}_+(x,z,s)$ is also expected to be square root singular as $x \downarrow 0^+$ for any z . This result can be used in conjunction with the Abelian theorem regarding asymptotic behaviour of Fourier transforms [6] to determine the asymptotic properties of $\Sigma_+(\xi;\zeta)$, namely,

$$\lim_{\xi \uparrow \infty} \sqrt{2\xi/s} e^{-i\pi/4} \Sigma_+(\xi;\zeta) = \lim_{x \downarrow 0^+} \sqrt{x} \hat{\sigma}_+(x,z,s). \quad (4.13)$$

Since the right hand side of (4.13) is equal, by (4.12), to a function parametric in s and ζ , $\Sigma_+(\xi;\zeta) = O(\xi^{-1/2})$ as $\xi \uparrow \infty$. Furthermore, u_- is expected to vanish as $x \uparrow 0^-$ and $|G_+(\xi;\zeta)| = O(|\xi|^{-1/2})$ as $|\xi| \uparrow \infty$. Therefore, both sides of (4.11) vanish as $|\xi| \uparrow \infty$. That is, $E(\xi) \rightarrow 0$ as $|\xi| \uparrow \infty$. From the preceding discussion it follows that $E(\xi)$ is a bounded function in the entire ξ plane. According to Liouville's theorem a bounded entire function is a constant [4], and therefore $E(\xi)$ must be identically

zero, i.e. $E(\xi) \equiv 0$. Equation (4.11) can now be solved for Σ_+ and U_- , which are found to be

$$U_-(\xi; \zeta) = \frac{P}{2\pi i v} \frac{b^2}{\mu \kappa} \frac{G_+(ic; \zeta) G_-(\xi; \zeta)}{\xi - ic} \quad (4.14)$$

$$\Sigma_+(\xi; \zeta) = -\frac{P}{2\pi i v} \frac{1}{(\xi - ic)} \left[\frac{G_+(ic; \zeta)}{G_+(\xi; \zeta)} - 1 \right]$$

This completes the formal solution of the problem. In theory, the exact solution to the problem is found by taking the triple inverse transforms of (4.14).

5. INVERSION

Unfortunately, an exact inversion of Σ_+ and U_- as given by (4.14) is not evident. This section is concerned with the determination of the stress intensity factor history, which is given by the asymptotic inversion of Σ_+ with respect to ξ . As mentioned in section 4, the asymptotic behaviour of $\Sigma_+(\xi; \zeta)$ as $|\xi| \uparrow \infty$ is intimately related to the behaviour of the double transform $\hat{\Sigma}_+(x, \zeta)$, of the normal stress $\sigma_+(x, z, t)$ as $x \downarrow 0^+$. It follows from (4.12) that the Laplace transform of the dynamic stress intensity factor history $k_I(t, z)$ is simply

$$\hat{K}_I(s, z) = \lim_{x \downarrow 0^+} \sqrt{2\pi x} \hat{\sigma}_+(x, z, s). \quad (5.1)$$

Thus, the double transform of $k_I(t, z)$ is found from (4.13) and (4.14) to be

$$\hat{K}_I(s, \zeta) = \frac{P}{\pi v} \sqrt{\pi/s} \frac{\sqrt{c + (\zeta^2 + a^2)^{1/2}}}{[c + (\zeta^2 + r^2)^{1/2}] S_+(ic, \zeta)}. \quad (5.2)$$

By construction, the function $\hat{K}_I(s, \zeta)$ is analytic on the strip $-ia < \zeta < ia$. Since the Wiener-Hopf factorization has been completed and the limiting process that resulted in $\hat{K}_I(s, \zeta)$ has suppressed all dependence on the variable ξ , there is no longer any need to restrict ζ to this strip. For the purposes of inverting this function it will be advantageous to extend the

definition of the function to the entire ζ plane. It is this extended function which is referred to as the Fourier transform of $\hat{k}_I(s,z)$. This function can be made single valued by cutting the ζ plane along $a < |\text{Im}(\zeta)| < \infty, \text{Re}(\zeta)=0$ and along $r < |\text{Im}(\zeta)| < \infty, \text{Re}(\zeta)=0$. This ensures that the square roots have positive real parts. The function $S_+(ic,\zeta)$ is analytic over the entire ζ plane by virtue of a theorem pertaining to analytic functions defined by integrals ([4], p. 92; [6], pp. 11-12).

The inverse Fourier transform of (5.2) is

$$\hat{k}_I(s,z) = \frac{s}{\sqrt{2\pi}} \int_{-\infty + i\zeta_0}^{\infty + i\zeta_0} \hat{k}_I(s,\zeta) e^{-is\zeta z} d\zeta \quad (5.3)$$

where ζ_0 is a real number between $-a$ and a . It is hoped that the final Laplace inversion of $\hat{k}_I(s,z)$ can be done by means of the convolution formula. Therefore, it will be advantageous to cast (5.3) in the form of a one sided Laplace transform so that the inversion can be performed by inspection. The required transformation can be achieved by suitably deforming the Fourier inversion path into a branch line integral; this is a trivial case of the Cagniard-deHoop technique. Consider the case of $z > 0$. For (5.3) to be a convergent integral when $z > 0$, it is necessary that the inversion contour lie in the lower half plane $\text{Im}(\zeta) < 0$. Since the finite ζ plane does not contain any singularities aside from the branch points at $\zeta = \pm ia$ and $\zeta = \pm ir$, the original inversion path can be deformed into a new contour as depicted in Figure 5. This new contour consists of two quarter

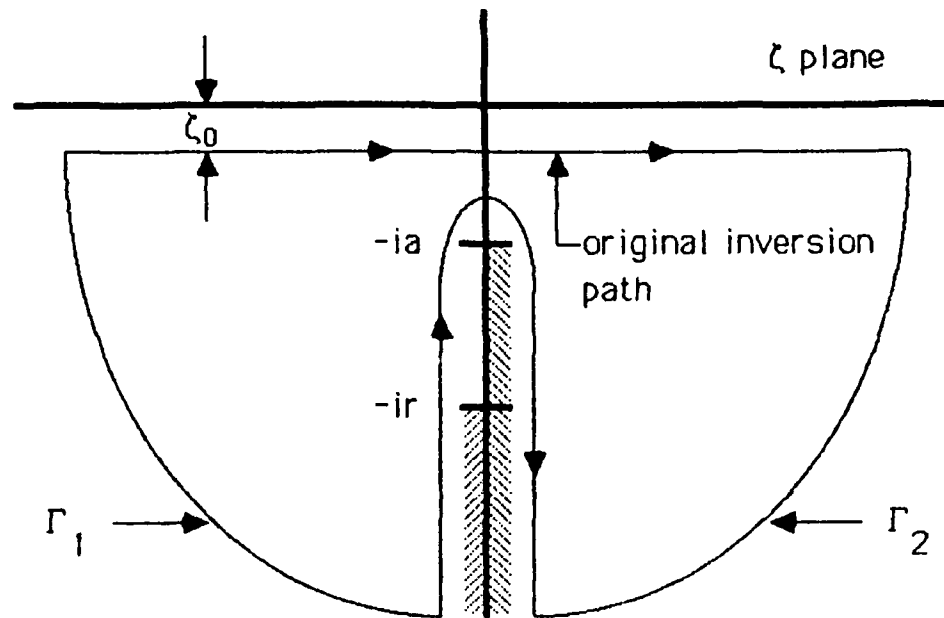


Figure 5. The complex ζ plane showing the singularities of $\hat{K}_1(s, \zeta)$ and the integration path for the evaluation of (5.3).

circles Γ_1 and Γ_2 in the lower half plane, and a branch line path running upward along the left hand side of the branch cut from $-i\infty$ up to the branch point at $\zeta = -ia$, around the branch point, and finally running down the right hand side of the branch towards $-i\infty$. That the original integral in (5.3) is equivalent to the integral of the same argument along the new path follows from Cauchy's integral theorem. This theorem states that the contour integral of a function which is analytic on and inside the contour is identically zero [4]. The contribution of the integral along the arcs at infinity Γ_1 and Γ_2 as $|\zeta| \rightarrow \infty$ vanishes by Jordan's Lemma [4]. Thus (5.3) reduces to a branch line integral. Exploiting the fact that $\hat{K}_1(s, -\bar{\zeta}) = \overline{\hat{K}(s, \zeta)}$, where the bar denotes complex conjugation, the branch line integral can be expressed, after an elementary change of variables, as

$$\hat{k}_1(s,z) = \frac{\sqrt{2} P}{\pi v} z^{-1} s^{-1/2} s \int_{az}^{\infty} e^{-s\eta} \operatorname{Im}\{F(+0+i\eta/z)\} d\eta \quad (5.4)$$

where

$$F(\zeta) = \frac{\sqrt{c+(\zeta^2+a^2)^{1/2}}}{[c+(\zeta^2+r^2)^{1/2}]S_+(ic,\zeta)} \quad (5.5)$$

In (5.4), $F(\zeta)$ is evaluated on the right hand side of the branch cut. The s -multiplied Laplace transform in (5.4) can be expressed as the Laplace transform of a derivative, i.e.

$$\hat{k}_1(s,z) = \frac{\sqrt{2} P}{\pi v} z^{-1} s^{-1/2} \int_{az}^{\infty} e^{-s\eta} \frac{\partial}{\partial \eta} \operatorname{Im}\{F(+0+i\eta/z)\} d\eta \quad (5.5)$$

There is no endpoint contribution from $\eta = az$ in (5.5), because $F(+0+ia)$ is a real quantity. The inversion of (5.5) is now obvious because $\hat{k}_1(s,z)$ is seen to be the product of two transforms. Therefore $k_1(t,z)$ is the convolution integral of the inverses of the two transforms,

$$k_1(t,z) = \frac{\sqrt{2} P}{\pi^{3/2} v} z^{-1} \int_a^{t/z} \frac{\partial}{\partial \zeta} \operatorname{Im}\{F(+0+i\zeta)\} \frac{d\zeta}{\sqrt{t-\zeta z}} H(t-az) \quad (5.6)$$

for $z > 0$, and $k_1(t,-z) = k_1(t,z)$. The expression for k_1 in (5.6) apparently cannot be reduced further in terms of elementary functions. Some of the properties of the real integral (5.6) along with an interpretation of the results are discussed in the next section.

6. CONCLUSION

Even though the dynamic stress intensity factor history (5.6) cannot be evaluated in terms of elementary functions it can be evaluated numerically and some of its salient features can be obtained analytically. Figures 6, 7, 8 and 9 show the results of the numerical integration of the integral (5.6) for the values of the ratio of the point load velocity to the Rayleigh wave speed of 0.8, 0.6, 0.4, and 0.2 for a Poisson ratio of $\nu=0.3$ ($c_l/c_r=2.02$). The time scale has been non-dimensionalized so that $\tau=1$ corresponds to the arrival of the dilatational wave at the observation position z along the crack front. The dynamic stress intensity factor has been normalized by premultiplying (5.6) by $P^{-1}(\pi z)^{3/2}$.

Following the sudden application of the point loads, a point z along the crack edge is at rest until the arrival of the dilatational front. This front is compressive in nature and the crack faces respond to it by initially trying to close together. This is reflected by the stress intensity factor being negative initially. The initial jump in the dynamic stress intensity factor, which can be seen in the graphs, is a verifiable feature of the solution of this particular three dimensional loading distribution. For the case of a pair of line loads acting perpendicular to the crack edge, i.e the convolution of the traction distribution (4.1) for $\nu=0$, Freund [1] found that the dynamic stress intensity factor started from zero and gradually became negative. By taking the limit as $t/z \downarrow a^+$ in (5.6) the jump is found to be

$$\lim_{t/z \downarrow a^+} k_I(t,z)(\pi z)^{3/2} p^{-1} = - \frac{\pi}{4} \frac{\sqrt{4ac}}{[c + \sqrt{r^2 - a^2}] S_+(ic, 0^+ + ia)} \quad (6.1)$$

The dynamic stress intensity factor becomes increasingly negative until the arrival of the Rayleigh waves at $\tau=2.02$ when it becomes logarithmically singular. Between $\tau=1$ and $\tau=2.02$, $k_I(t,z)$ also exhibits a disturbance coinciding with the arrival of the shear front at $\tau=1.88$. This mild discontinuity in the slope of $k_I(t,z)$ is due to a change in the form of the function S_+ as the branch point located at the shear wave slowness is crossed. After the passage of the Rayleigh waves the crack faces begin to open, the stress intensity factor increases until reaching a maximum, and thereafter decaying very gradually towards its limiting value $k_I(\infty, z)=0$.

This completes the analysis of the three dimensional stress intensity factor history for the case of a pair of moving point loads on the faces of a crack. The solution (5.6) to the problem described by the traction distribution (4.1) is the fundamental solution to the class of problems involving traction distributions moving perpendicular to the crack edge. In this paper the range of applicability of the procedure introduced by Freund [1] has been successfully extended to this class of problems. Other situations, such as moving loads along a direction inclined to the crack edge, can be examined following the same methodology used in this paper.

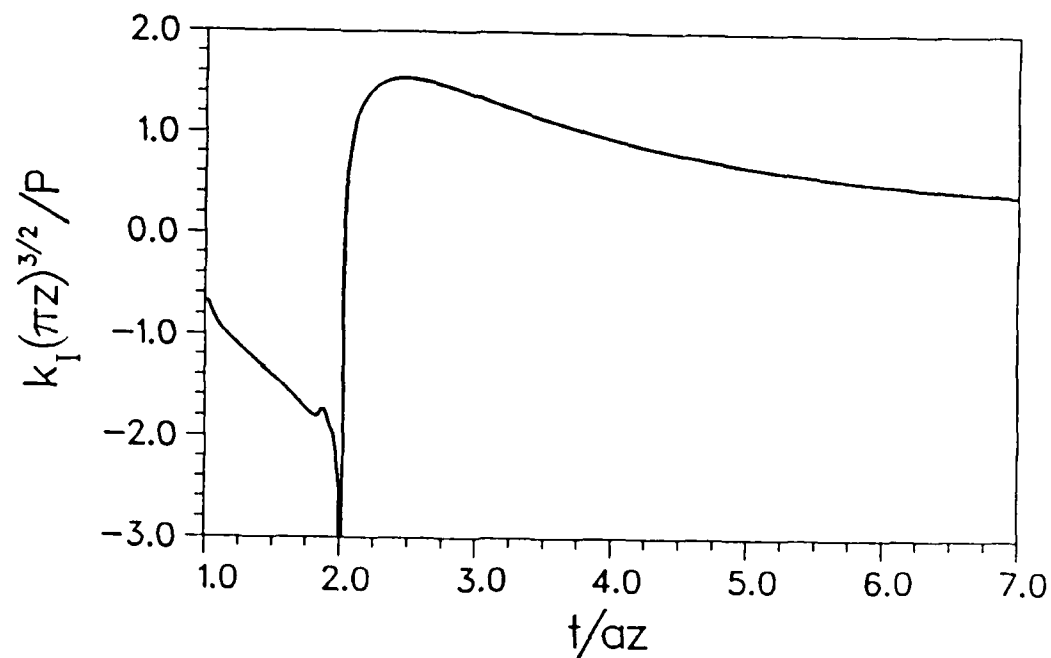


Figure 6. The normalized stress intensity factor $k_I(t,z) (\pi z)^{3/2} p^{-1}$ versus t/az for the case of $c/r = 0.8$.

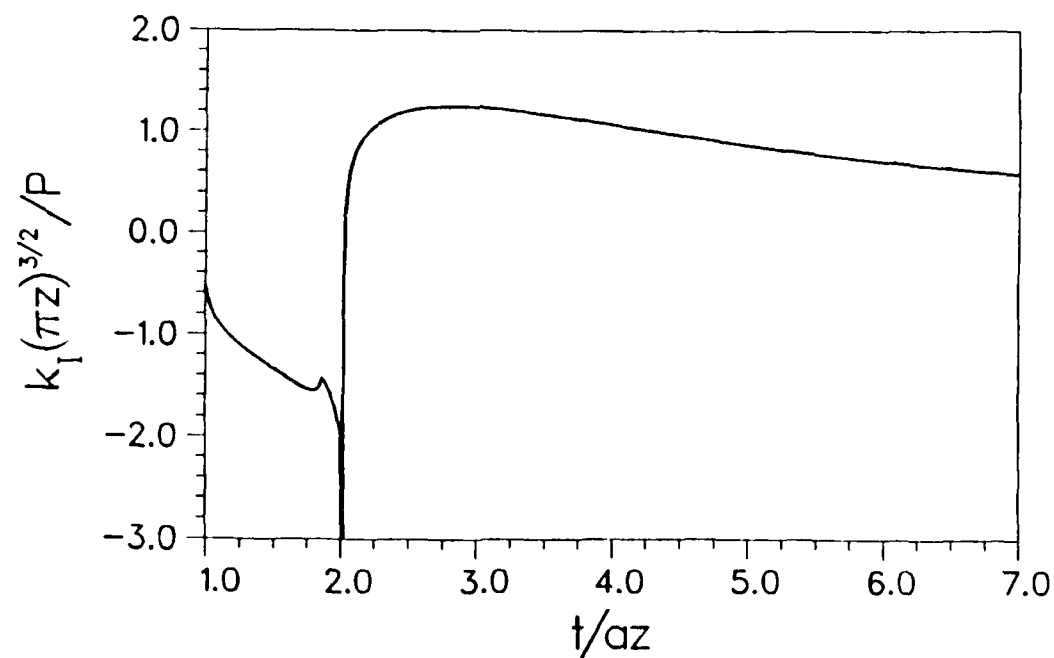


Figure 7. The normalized stress intensity factor $k_I(t,z) (\pi z)^{3/2} p^{-1}$ versus t/az for the case of $c/r = 0.6$.

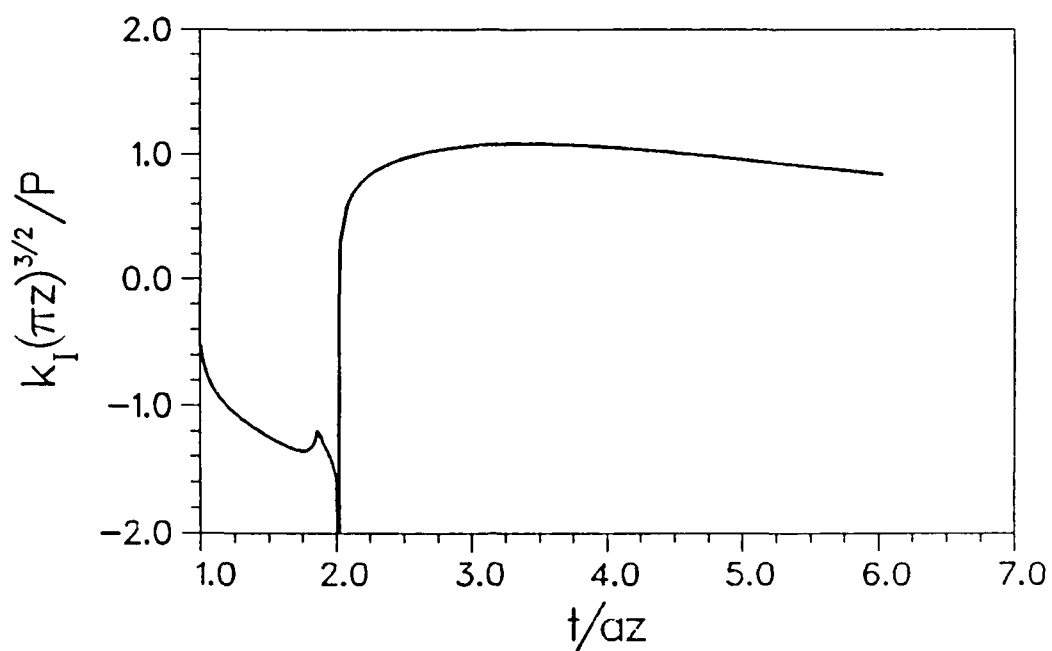


Figure 8. The normalized stress intensity factor $k_I(t,z) (\pi z)^{3/2} p^{-1}$ versus t/az for the case of $c/r = 0.4$.

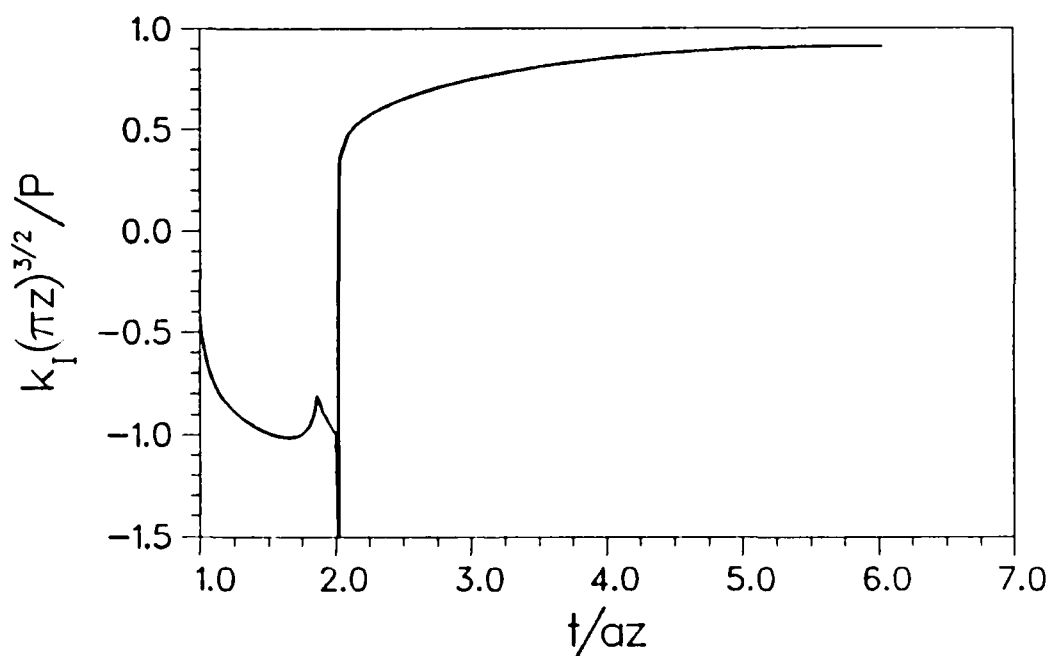


Figure 9. The normalized stress intensity factor $k_I(t,z) (\pi z)^{3/2} p^{-1}$ versus t/az for the case of $c/r = 0.2$.

APPENDIX

In this appendix the factorization of the function $S(\xi; \zeta)$ as defined by (4.6) is carried out. As mentioned in section 4, the function $S(\xi; \zeta)$ has no zeros or poles in the ξ plane cut along $\bar{a} < |\operatorname{Im}(\xi)| < \bar{b}$, $\operatorname{Re}(\xi) = 0$. Furthermore, the function $S(\xi; \zeta)$ has the desired property of being asymptotic to unity as $|\xi| \uparrow \infty$. These properties enable one to factorize $S(\xi; \zeta)$ into the product $S_+(\xi; \zeta)S_-(\xi; \zeta)$ by a well known decomposition technique ([6], pp. 15-17). Specifically, one considers the Cauchy integral representation for $\ln S(\xi; \zeta)$, that is, one represents $\ln S(\xi; \zeta)$ by the following contour integral

$$\ln S(\xi; \zeta) = \frac{1}{2\pi i} \oint_{\Gamma} \ln S(\vartheta; \zeta) \frac{d\vartheta}{\vartheta - \xi}. \quad (\text{A1})$$

The counterclockwise contour Γ is depicted in Figure 10. By expanding the contour Γ to infinity, making use of the asymptotic behaviour of $S(\xi; \zeta)$, an equivalent representation of (A1) is obtained. The integral (A1) around the contour Γ at infinity is equivalent to two clockwise contours Γ_+ and Γ_- around the branch cuts as shown in Figure 10, so that

$$\ln S(\xi; \zeta) = \ln S_+(\xi; \zeta) + \ln S_-(\xi; \zeta) = \frac{1}{2\pi i} \oint_{\Gamma_+ + \Gamma_-} \ln S(\vartheta; \zeta) \frac{d\vartheta}{\vartheta - \xi}. \quad (\text{A2})$$

Thus, the functions $S_+(\xi; \zeta)$ and $S_-(\xi; \zeta)$ are given by

$$S_{\pm}(\xi; \zeta) = \exp \left[\frac{1}{2\pi i} \oint_{\Gamma_{\pm}} \ln S(\gamma; \zeta) \frac{d\gamma}{\gamma - \xi} \right]. \quad (A3)$$

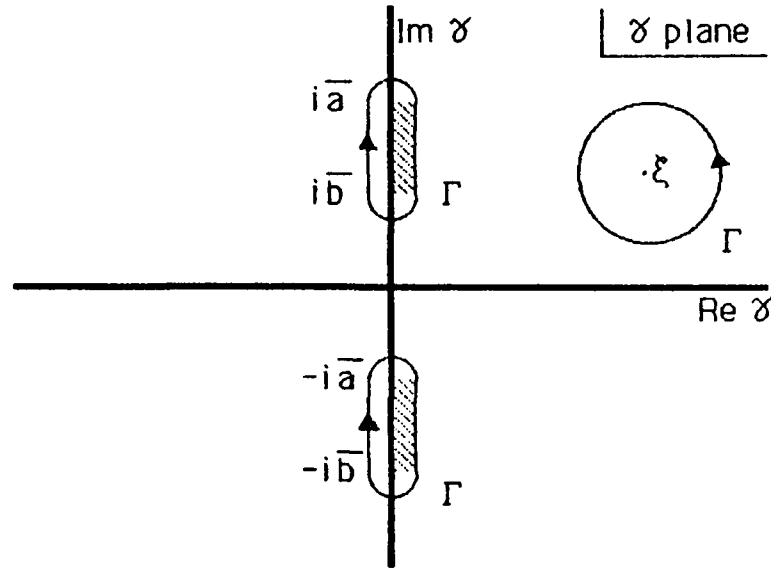


Figure 10. The complex γ plane showing the singularities of $S(\gamma; \zeta)$ and the integration path for the evaluation of (A.1).

As can be seen from (A3) and Figure 10, the functions $S_+(\xi; \zeta)$ and $S_-(\xi; \zeta)$ are analytic and nonzero in the half planes $\text{Im}(\xi) > -\bar{a}$ and $\text{Im}(\xi) < \bar{a}$, respectively. It remains to evaluate the contour integrals.

For illustrative purposes consider the function $S_+(\xi; \zeta)$. Along the right hand side of Γ_+ , i.e. $-\bar{b} < \text{Im}(\xi) < -\bar{a}$, $\text{Re}(\xi) = 0^+$, the Rayleigh wave function (3.13) has the explicit form

$$R(0^+ + i\gamma; \zeta) = (\bar{b}^2 + \zeta^2 - 2\gamma^2)^2 + 4i(\zeta^2 - \gamma^2)[(\gamma^2 - \bar{a}^2)(\bar{b}^2 - \gamma^2)]^{1/2} \quad (A4)$$

where $\vartheta = \text{Im}(\xi)$. Along the left hand side of Γ_+ , $R(\xi; \zeta)$ is given by the complex conjugate of (A4). From (4.6)

$$\ln S(\xi; \zeta) = \ln R(\xi; \zeta) - \ln[2(b^2 - a^2)(\bar{r} + \xi^2)] \quad (\text{A5})$$

and therefore $S_+(\xi; \zeta)$ can be expressed as,

$$\ln S_+(\xi; \zeta) = \frac{1}{2\pi} \int_{-\bar{a}}^{-\bar{b}} \frac{\ln R(+0+i\vartheta)}{i\vartheta - \xi} d\vartheta - \frac{1}{2\pi} \int_{-\bar{a}}^{-\bar{b}} \frac{\ln R(-0+i\vartheta)}{i\vartheta - \xi} d\vartheta \quad (\text{A6})$$

$$= \frac{1}{2\pi} \int_{-\bar{a}}^{-\bar{b}} \ln \left[R(+0+i\vartheta)/R(-0+i\vartheta) \right] \frac{d\vartheta}{i\vartheta - \xi} \quad (\text{A7})$$

$$= \frac{i}{\pi} \int_{\bar{a}}^{\bar{b}} \tan^{-1} \left[\frac{4(\zeta^2 - \vartheta^2)[(\vartheta^2 - \bar{a}^2)(\bar{b}^2 - \vartheta^2)]^{1/2}}{(\bar{b}^2 + \zeta^2 - 2\vartheta^2)^2} \right] \frac{d\vartheta}{i\vartheta + \xi} \quad (\text{A8})$$

The function $S_-(\xi; \zeta)$ is treated similarly. One further change of variables $\eta = (\vartheta^2 - \zeta^2)^{1/2}$ reduces (A8) to the form (4.7).

ACKNOWLEDGMENTS

I would like to extend my gratitude to Professor L. B. Freund for suggesting the problem treated in this paper. Some helpful conversations with Dr. C. Champion, J. Leighton and G. Ravichandran are gratefully acknowledged. The research was possible thanks to the National Science Foundation, Solid Mechanics Program Grant No. MSM-85-13096, and the Office of Naval Research contract N00014-85-k-0597 which provided access to the NRL Central Computer Facility.

REFERENCES

- [1] L. B. Freund, *The Stress Intensity Factor History due to Three Dimensional Transient Loading of the Faces of a Crack*, Journal of the Mechanics and Physics of Solids (to appear), (1986).
- [2] D. D. Ang, *Elastic Waves Generated by a Force Moving Along a Crack*, Journal of Mathematics and Physics 38, pp. 246-256, (1960).
- [3] D. C. Gakenheimer and J. Miklowitz *Transient Excitation of an Elastic Half Space by a Point Load Traveling on the Surface*, Journal of Applied Mechanics 3, pp. 505-515, (1969).
- [4] E. T. Whittaker and G. N. Watson, *A Course of Modern Analysis*, Cambridge University Press, 1927.
- [5] J. D. Achenbach, *Wave Propagation in Elastic Solids*, North-Holland, 1973.
- [6] B. Noble, *Methods Based on the Wiener-Hopf Technique*, Pergamon, Oxford, 1958.

END

DTIC

8-86